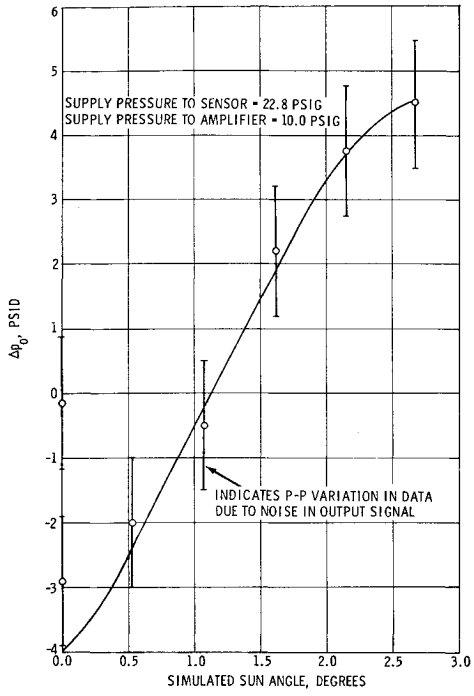

Fig. 3 Fluidic sun sensor over-all calibration.

material used was plexiglass, 0.062 in. thick with a cutting depth of 0.050 in. The inlet restrictors consist of two plates, each containing four 0.005-in.-diam orifices, 0.031 in. apart.

During testing of the fluidic sun sensor, there was a slight mismatch in pressure drops on the two sides of the detector, and as a result, null signal corresponded to the high end of the unilateral differential-pressure gage monitoring the sun sensor output signal. The range of the gage null adjustment was sufficient to enable nulling in one direction, but not in the other. Therefore, data were obtained in one direction only as indicated in the data plotted for steady-state sun sensor performance in Fig. 2. The linear range is shown to be about $\pm 3.0°$. The supply pressure to the detector element was 22.8 psig, while the pressure just downstream of the detector inlet restrictors was about 0.25 psig at null signal. A slight mismatch (null offset) is understandable in this situation where the output differential pressure is read in tenths of an inch of water. This is a much more stringent operating condition than that to be encountered in a space application where ambient pressure would be practically zero rather than 14.7 psia. Since the inlet restrictor must be choked, the supply pressure (absolute) must be at least twice the absolute output pressure, hence the 22.8 psig (37.5 psia) supply for lab testing.

In the laboratory, the inlet restrictor pressure drop is about 22.5 psi. A difference of 1% in the pressure drops across the two "parallel" inlet restrictors corresponds to a null offset of 6.2 in. of water. In space, where the inlet restrictor pressure drop would be about 0.50 psi, a 1% mismatch represents a null offset of 0.1 in. of water. This is better than an order-of-magnitude improvement in matching requirements.

After completing the testing of the breadboard model as previously described, additional testing was conducted with the detector output connected to a high-gain fluid amplifier. It was expected that a high-gain amplifier would be required to bring the signal strength, i.e., the over-all sun sensor gain, up to a level compatible with fluidic circuitry. The results of this test are presented in Fig. 3. The null offset is attributed primarily to the detector as previously mentioned. The noise band indicated is based on observations of the pressure gage fluctuations and cannot be considered more than indicative of what the noise might be if measured rigorously.

References

[1] Miller, W. V., "Fluidic Sun Sensor for Solar-Pointing Fluidic Attitude Control," *Proceedings of the 1969 Joint Automatic Control Conference*, AIAA, Boulder, Colo., 1969.

[2] Garner, H. D. and Fuller, H. V., Jr., "A Survey of Potential Applications to Spacecraft Attitude Control," *Proceedings of the 1966 SAE Fluidics Symposium*, Society of Automotive Engineers, 1966.

Like and Unlike Impinging Injection Element Droplet Sizes

R. A. Dickerson*
Rocketdyne, A Division of North American Rockwell Corporation, Canoga Park, Calif.

THIS study of the measurement of spray droplet sizes by a frozen wax technique was a portion of a larger study[1] on the combustion of sprays. Of a number of prior studies using particle freezing techniques (e.g., Ref. 2–4), the work by Joyce[4] was most applicable to the present study. The liquid paraffin wax he sprayed from fuel atomizer nozzles gave frozen particles that were sticky and tended to sinter upon standing. As a result, particle sieving operations were laboriously carried out by hand, using a stream of water to separate the particles and induce them to pass through each screen. We improved his technique by using a better-suited wax and extended it to the study of sprays from unlike impinging injector elements (i.e., fuel impinging on oxidizer as in unlike doublet or four-on-one injector elements) by using both heated water and molten wax as propellant simulants.

Some initial tests were made with food-preserving paraffin wax which had a melting point of 130°F and a block point temperature (the temperature at which two wax-coated surfaces stick together sufficiently to mar either surface) of 90°F. This wax yielded particles that had good sphericity but were sticky enough to make sieving difficult. In contrast, Type 270 wax, a product of the Petrochemicals Division of Shell Chemical Company, with a melting point of 140°F, and a block point temperature of 120°F gave particles having equally good sphericity but the particles were not sticky and had sieving characteristics comparable to dry sand. Figure 1 shows photomicrographs of two sieve cuts from one test.

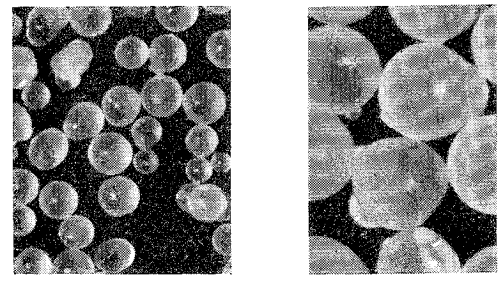

a) b)

Fig. 1 Photomicrographs of wax particle sieve cuts: a) 0–125μ; b) 250–297 μ.

Received January 6, 1969; revision received July 18, 1969. This work was performed under AFRPL Contract AF04(611)-67-C-0081.

* Member of the Technical Staff, Research Division.

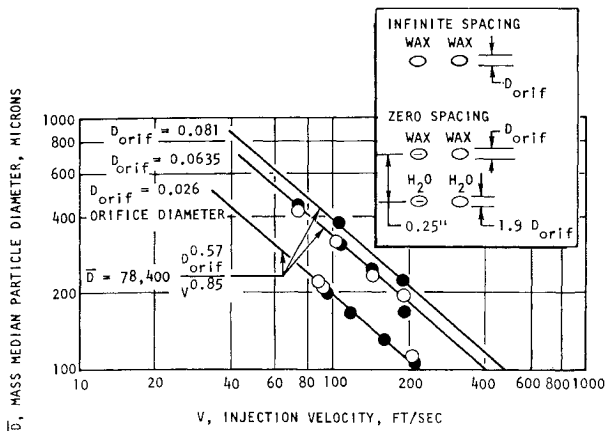

Fig. 2 Mass median particle sizes for like-doublet injectors, obtained using the frozen wax technique. Open symbols are zero spacing and closed symbols are infinite spacing.

Experimental Apparatus

Three impinging stream injector types were used in the experiments: like doublets, unlike doublets, and four-on-one unlike quintuplets. The drilled orifices for all injectors had rounded entrances and an L/D (length/diameter ratio) of 10 to minimize effects of flow separation at orifice entrances. Impingement distance for all of the injector designs was selected so that the freestream L/D was in range 4 to 8. The like doublet and unlike doublet injectors all had 60° impingement angles. The unlike quintuplets also had 60° included angle between opposing oxidizer streams (30° angle between the central fuel orifice and the outer four oxidizer orifices).

The wax and water supply tanks each consisted of lengths of 2-in.-diam stainless-steel tubing, immersed in a hot-water bath that was heated by thermostatically controlled electrical heaters and stirred by a nitrogen bubbler. A shroud enclosed the top of the water bath and the injector, so that the liquid feed lines, injector, and spray formation zone were heated by condensing water vapor and hot N_2 from the bubbler. This warm environment assured that the wax did not freeze prior to completion of the atomization process. For collection of the sprayed particles, a 20- × 30-ft plastic-coated canvas sheet was suspended from the ceiling in a catenary shape. The orientation of the injectors was such that the liquid wax spray became frozen during flight, before landing on the canvas.

Experimental Procedures

For each test, system temperature was 200–205°F and spraying was continued for at least 10 sec, or until ~2 lb of frozen wax particles were produced. After each test the particles were washed from the canvas sheet with tap water, collected, and temporarily stored in plastic bags. Wash water was removed from the samples by placing them in a vacuum chamber for a period of at least 48 hr, after initial drying by suction filtration.

To obtain particle size distributions, 20-g samples of the collected wax particles were sieved, using standard testing sieves and a Ro-Tap sieve shaker. Data obtained from the sieving were converted into terms of the total fraction of mass having a particle size smaller than each of the sieve sizes, and the particle size for each test characterized by a single number, the mass median particle diameter $\bar{D}$, the particle diameter for which the cumulative weight fraction is equal to 0.5. No particle diameter correction was made to account for wax density change (from 0.79 to 0.92) upon freezing, because air bubbles entrapped in the particles approximately compensated for the density change.

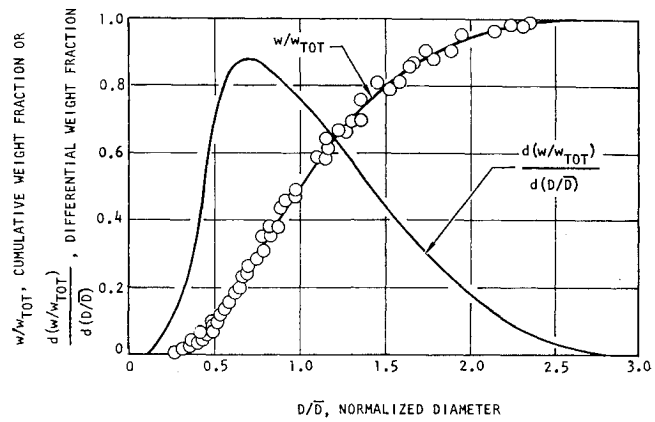

Fig. 3 "S" curve and bell curve obtained by differentiation of the "S" curve. Like doublets with zero spacing.

Experimental Data and Correlations

Like-doublet results

Seventeen tests were conducted using like-doublet injector elements. The wax particles obtained for all of the like-doublet tests were of good quality, similar to particles obtained during the feasibility tests.

For six of the like doublet tests, pairs of spray fans were used, one of molten wax, and one of hot water, both in the same geometrical plane (to simulate a fuel fan very close to an oxidizer fan); and, for the remaining 11 tests, only the wax fan was used. The tests using both fans are referred to as having zero spacing between fuel and oxidizer spray fan planes, and those with only the wax spray fan are referred to as having infinite spacing. For zero spacing the water orifice diameters were always 1.9 times as large as the wax orifice diameters, and water injection pressure was equal to the wax injection pressure.

The like-doublet particle size data are plotted as a function of injection velocity and orifice diameter in Fig. 2. It is concluded that spacing does not have an appreciable effect on the mass median particle diameter, and the data were therefore curve-fitted by the means of least squares, to the following equation:

$$\bar{D} = 7.84 \times 10^4 D^{0.57}_{\text{orif}}/V^{0.85} \qquad (1)$$

where $\bar{D}$ = mass median particle diameter, μ; D_{orif} = wax orifice diameter, in.; and V = wax injection velocity, fps. It was found that the particle size distribution data obtained for all like-doublet tests with zero spacing, and all like-doublet tests with infinite spacing could be normalized into two characteristic particle size distribution curves by plotting for each test the cumulative weight fraction of particles vs

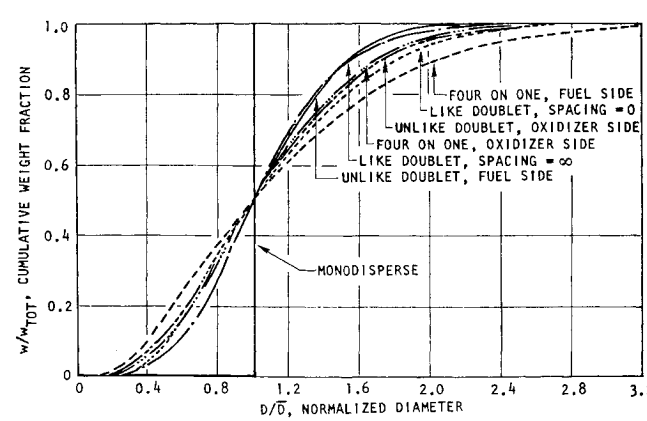

Fig. 4 Normalized particle distribution curves for the injector element types investigated.

Table 1 Particle size distribution function parameters

		General exponential				Rosin-Rammler
		A	B	C	δ	Γ
Like doublets, zero spacing	1450	5.00	7.45	0.772	2.45	1.26
Like doublets, infinite spacing	5.65	2.78	1.77	1.78	2.84	1.20
Unlike doublets, fuel side	1.64	1.57	0.575	2.89	2.67	1.15
Unlike doublets, oxidizer side	4.44	2.14	1.68	1.58	2.46	1.21
Four-on-one, fuel side	1.65×10^7	6.07	17.0	0.404	2.03	1.34
Four-on-one, oxidizer side	7.28	2.47	2.18	1.38	2.46	1.24

the quotient of particle diameter to the mass median particle diameter ($D/\bar{D}$). Data of $D/\bar{D}$ vs cumulative weight fraction for all like-doublet tests with zero spacing were found to fall on the normalized "S" curve shown in Fig. 3. This is significant, because for an injector with infinite spacing $\bar{D}$ can be calculated from Eq. (1) and used with Fig. 3 to obtain the complete particle distribution. It was similarly found that the particle distribution data from the zero spacing like-doublet tests could be normalized into one curve (Fig. 4).

The normalized distribution curve data were curve fitted by least squares to the Rosin-Rammler, general exponential, Nukiyama-Tanasawa, log probability, and upper limit distribution functions. These functions are discussed in detail in Ref. 1. It was found that the general-exponential function gave the best fits of the data, and the Rosin-Rammler function gave the second best fit. Shown in Table 1 are the numerical parameters for these curve-fitted distribution functions.

General exponential:

$$\frac{d(w/w_{\text{tot}})}{d(D/\bar{D})} = A\left(\frac{D}{\bar{D}}\right)^B \exp\left[-C\left(\frac{D}{\bar{D}}\right)^E\right] \tag{2}$$

Rosin-Rammler:

$$\frac{d(w/w_{\text{tot}})}{d(D/\bar{D})} = \frac{\delta(D/\bar{D})^{\delta-1}}{\Gamma^\delta} \exp\left[-\left(\frac{D/\bar{D}}{\Gamma}\right)^\delta\right] \tag{3}$$

where A, B, C, E, Γ, δ = curve fit parameters; $D/\bar{D}$ = particle diameter divided by mass median particle diameter; w/w_{tot} = cumulative weight fraction of particles having diameter smaller than D.

Unlike-doublet results

Twenty-two tests were conducted using unlike-doublet elements. The wax particles obtained for most tests, particularly the tests with high injection velocities, were of lower quality than obtained from the like-doublet tests. The particles had somewhat poorer sphericity, presumably because of effects due to the simultaneous use of wax and water as propellant simulants.

For the unlike-doublet tests, wax and water were used simultaneously as propellant simulants. For any particular test, wax was flowed through one orifice of the unlike-doublet element and water was flowed through the opposing orifice. For unlike-doublet elements, the fuel orifice diameter was generally smaller than or equal to the oxidizer orifice diameter. Fuel orifice diameters ranged from 0.026 to 0.159 in., and oxidizer diameters ranged from 0.035 to 0.213 in. Injection velocities ranged from 65 to 215 fps.

For all unlike-doublet tests with the wax orifice diameter equal to or less than the water orifice diameter, the particle distributions obtained represent fuel droplet distributions, and the following equation for fuel droplet sizes was obtained:

$$\bar{D}_f = 1.00 \times 10^5 \left[\frac{D_f^{0.27} D_o^{0.023}}{V_f^{0.74} V_o^{0.33}}\right]; \quad D_f \leq D_o \tag{4}$$

where $\bar{D}_f$ = mass median particle diameter for the fuel, μ; D_f, D_o = fuel and oxidizer orifice diameters, in.; and V_f, V_o = fuel and oxidizer injection velocities, fps. The tests for which the wax orifice diameter was larger than or equal to the water orifice diameter gave oxidizer particle size distributions, and the following equation was obtained:

$$\bar{D}_o = \frac{1.92 \times 10^6}{D_o^{0.38} V_o^{0.86} V_f^{1.19}}; \quad D_0 \geq D_f; \quad D_f = 0.0635 \text{ in.} \tag{5}$$

where $\bar{D}_o$ = mass median particle diameter for the oxidizer, μ. Note that D_f is not included in Eq. (5) since the limited amount of data for oxidizer dropsize were obtained with a constant D_f (0.0635 in.).

It was found that unlike-doublet particle size distribution functions could also be normalized into single curves, with a separate normalized curve for fuel and for oxidizer distributions (Fig. 4, Table 1).

Four-On-One Results

Twenty-eight tests were conducted using four-on-one unlike quintuplet injector elements. The wax particles obtained for these tests were, in general, of poorer quality than the particles obtained for either the unlike doublets or the like doublets. This poorer quality was probably a result of the stronger interaction between water and wax simulants which occurs when four-on-one elements are used. For 19 of the tests, wax was injected through the center (fuel) orifice, and water through the outer four orifices, to determine D_f distributions. For the remaining 9 tests, the simulants were reversed to determine D_o distributions. Fuel and oxidizer orifice diameters ranged from 0.025 to 0.086 in., and injection velocities ranged from 55 to 255 fps.

Least-squares curve fitting of the particle size data resulted in the following expressions for mass median particle diameters.

Center stream (fuel side):

$$\bar{D}_f = 3.61 \times 10^4 \left[\frac{D_f^{0.10} D_o^{0.12}}{V_f^{0.086} V_o^{0.89}}\right] \tag{6}$$

Outer streams (oxidizer side):

$$\bar{D}_o = 1.62 \times 10^5 \left[\frac{D_o^{0.68}}{V_o^{0.56} V_f^{0.57} D_f^{0.35}}\right] \tag{7}$$

Distinctly different normalized distribution curves (Fig. 4, Table 1) were obtained for the fuel and the oxidizer.

References

[1] Dickerson, R. A., Tate, K. W., and Barsic, N. J., "Correlation of Spray Injector Parameters with Rocket Engine Performance," AFRPL TR-68-147 (R-7499) June 1968, Rocketdyne, a Division of North American Rockwell Corp., Canoga Park, Calif.

[2] Weiss, M. A. and Worsham, C. H., "Atomization in High Velocity Air Streams," *ARS Journal*, Vol. 29, No. 4, April 1959, pp. 252–259.

[3] Wolfe, H. E. and Andersen, W. H., "Kinetics, Mechanism, and Resultant Droplet Sizes of the Aerodynamic Breakup of Liquid Drops," 0395-04(18)S, (AD43740), April 1964, Aerojet General Corp., Downey, Calif.

[4] Joyce, J. R., "The Wax Method of Spray Particle Size Measurement," TR I.C.T./7, Aug. 1946, Shell Petroleum Co., Ltd., Norman House, Strand, London.